

# Modeling of the Thermoelectric Properties of p-Type IrSb<sub>3</sub>

Jean-Pierre Fleurial

Jet Propulsion Laboratory/California Institute of Technology  
4800, Oak Grove Drive, MS 277-212, Pasadena, CA 91109

☎ 818-354-4144

Fax 81 X-393-6951

## ABSTRACT

IrSb<sub>3</sub> is a compound of the skutterudite family of materials [1,2] now being investigated at the Jet Propulsion Laboratory (JPL). A combination of experimental and theoretical approaches has been recently applied at JPL to evaluate the potential of several thermoelectric materials such as n-type and p-type Si<sub>80</sub>Ge<sub>20</sub> alloys, n-type and p-type Bi<sub>2</sub>Te<sub>3</sub>-based alloys and p-type Ru<sub>2</sub>Ge<sub>3</sub> compound [3-7]. The use of a comprehensive model for the thermal and electrical transport properties of a given material over its full temperature range of usefulness is a powerful tool for guiding, experimental optimization of the composition, temperature and doping level as well as for predicting the maximum ZT value likely to be achieved. Expressions for all the transport properties of thermoelectric semiconductors were derived from the Boltzmann's transport equation, using the relaxation time approximation. This widely used method has been employed with Fermi statistics to calculate carrier mobility, electrical conductivity, carrier concentration, Hall coefficient, Seebeck coefficient, electronic and bipolar contribution to the thermal conductivity as well as other transport coefficients in p-type IrSb<sub>3</sub>. The effect of minority carrier conduction was taken into account and the two most common carrier scattering mechanisms usually necessary to describe the transport properties in these heavy doping conditions were selected - acoustic phonon scattering and ionized impurity scattering. Determination of the lattice thermal conductivity of IrSb<sub>3</sub> was conducted by considering phonon-phonon, carrier-phonon and point defect scattering mechanisms. Calculations for the introduction of resonant scattering impurities and ultrafine inert scattering centers have also been performed to evaluate possible additional improvements in ZT.

## INTRODUCTION

The IrSb<sub>3</sub> compound has been recently investigated for its interesting thermoelectric properties [1,2]. The JPL study is part of an on-going search for new materials with the potential for high ZT values and substantial improvements in performance over current state of the art materials. This material belongs to a series of

compounds with the skutterudite structure with a rather complex unit cell of 32 atoms. Several of these compounds possess high p-type mobility values and it was of interest to develop a transport properties model for these materials.

High  $ZT$  values were reported by JPL on samples heat-treated in dynamic vacuum. Additional material analysis revealed that the surface of these samples partially decomposed into a high Seebeck coefficient, high electrical resistivity  $\text{IrSb}_2$  layer. The measurement techniques used were not deemed suitable for this type of composite samples and moreover, experimental results were very difficult to explain by any theoretical analysis [1]. As a consequence, the only experimental data considered for these calculations were results obtained on p-type  $\text{IrSb}_3$  single phase polycrystalline samples which were not heat-treated at elevated temperatures in a dynamic vacuum.

The use of a comprehensive model for the thermal and electrical transport properties of a given material over its full temperature range of usefulness is a powerful tool for guiding experimental optimization of the composition, temperature and doping level as well as for predicting the maximum  $ZT$  value likely to be achieved. This approach has already been used at JPL, to evaluate the potential of several thermoelectric materials such as n-type and p-type  $\text{Si}_{80}\text{Ge}_{20}$  alloys, n-type and p-type  $\text{Bi}_2\text{Te}_3$ -based alloys and p-type  $\text{Ru}_2\text{Ge}_3$  compound [3-7]. Building on results achieved for Si-Ge alloys and  $\text{PbTe}$ -based materials, the effect of two particular "engineered" scattering mechanisms on the maximum figure of merit has been studied.

## TRANSPORT PROPERTIES MODEL

### Electrical Properties

Expressions of all the transport properties of thermoelectric semiconductors were derived from the Boltzmann's transport equation, using the relaxation time approximation, as described in [8]. This widely used method has been employed with generalized Fermi statistics to calculate carrier mobility, electrical conductivity, carrier concentration, Hall coefficient, Seebeck coefficient, electronic and bipolar contribution to the thermal conductivity as well as other transport coefficients. The effect of minority carrier conduction (electrons in p-type  $\text{IrSb}_3$ ) was taken into account by the model: up to two conduction bands and two valence bands were considered. The two most common carrier scattering mechanisms usually necessary to describe the transport properties in the low heavy doping conditions were selected: acoustic phonon scattering and ionized impurity scattering of the charge carriers. The total charge carrier scattering rate for a given band  $(\tau_{sc})^{-1}$  can be expressed as:

$$\frac{1}{\tau_b} = \frac{1}{\tau_{ac}^b} + \frac{1}{\tau_{ion}^b} \quad (1)$$

where  $\tau_{ac}^b$  is the relaxation time due to acoustic phonons and  $\tau_{ion}^b$  is the relaxation time due to ionized impurities. Expressions for these relaxation times and equations for the calculation of the various electrical transport parameters were given earlier [5].

## Lattice Thermal Conductivity

Calculation of the lattice thermal conductivity was carried out by using the Boltzmann's equation for phonons considering three phonon scattering mechanisms: normal and Umklapp phonon-phonon scattering, point defect scattering and carrier-phonon scattering. The expression for the total phonon scattering rate  $(\tau_c)^{-1}$  can be expressed as:

$$\frac{1}{\tau_c} = \frac{1+\beta}{\tau_u} + \frac{1}{\tau_{pd}} + \frac{1}{\tau_c} \quad (2)$$

where  $\tau_u$  is the relaxation time due to three-phonon Umklapp processes,  $\beta$  is the ratio of the Umklapp to normal phonon-phonon relaxation,  $\tau_{pd}$  is the relaxation time due to point defect scattering and  $\tau_c$  is the relaxation time due to carrier-phonon scattering. Expressions for these relaxation times and equations for the calculation of the lattice thermal conductivity were given earlier [5].

## Fit to experimental data

The experimental data sets to be fitted consisted of a number  $n$  of data points providing temperature  $T$ , composition, electrical conductivity  $\sigma$ , Hall mobility  $\mu_H$ , Seebeck coefficient  $S$ , thermal conductivity  $\lambda$  and dimensionless figure of merit  $ZT$  [7]. Determination of the adjustable parameters was achieved by minimizing the statistical  $\chi^2$  function in (3), using a generalized non-linear square fit technique:

$$\chi^2 = \sum_{i=1}^n w_i^\sigma \left(1 - \frac{\sigma_i^{\text{exp}}}{\sigma_i}\right)^2 + \sum_{i=1}^n w_i^\mu \left(1 - \frac{\mu_i^{\text{exp}}}{\mu_i}\right)^2 + \sum_{i=1}^n w_i^S \left(1 - \frac{S_i^{\text{exp}}}{S_i}\right)^2 + \sum_{i=1}^n w_i^\lambda \left(1 - \frac{\lambda_i^{\text{exp}}}{\lambda_i}\right)^2 + \sum_{i=1}^n w_i^{ZT} \left(1 - \frac{Z_i T_i^{\text{exp}}}{Z_i T_i}\right)^2 \quad (3)$$

where the different weighting factors  $w_i$  are equal to 1 or 0 depending on whether the corresponding experimental data is or is not known. The total number of degrees of freedom  $N_{DF}$  indicates to what extent the fit is overdetermined; and is calculated as the total number of experimental properties provided plus 1, reduced by the total number of adjustable parameters:

$$N_{DF} = \sum_{i=1}^n w_i^c + \sum_{i=1}^n w_i^u + \sum_{i=1}^n w_i^s + \sum_{i=1}^n w_i^\lambda + \sum_{i=1}^n w_i^{ZT} + 1 - (n_{adj} + n) \quad (4)$$

The electrical resistivity, Seebeck coefficient, Hall mobility, thermal diffusivity and heat capacity of several good quality samples was measured in the 25-600°C temperature range. These samples had a large grain microstructure (>30 μm) and were close to the theoretical density (about 90-95%) [1].

A single least-square fit simultaneously applied to all of the selected p-type IrSb<sub>3</sub> experimental data (66 data points from 6 samples) resulted in a root-mean-square deviation between the calculated and observed values of about ±2%. This good agreement was obtained by considering a one valence band, one conduction band structure and only six adjustable parameters, which are reported in Table 1. Except for the effective masses  $m_p^*$  and  $m_n^*$ , all other parameters were fixed equal in value.

Table 1: Adjustable transport parameters determined from fitting p-type IrSb<sub>3</sub> experimental data.

$m_p^*$	$m_n^*$	$E_d$	$\epsilon$	$\gamma$	$\beta$
0.134 $m_0$	2.00 $m_0$	16.56 eV	29788	3.72	2

The low value obtained for the hole effective mass  $m_p^*$  is consistent with the very large mobilities and moderate Seebeck coefficients of p-type IrSb<sub>3</sub>.  $E_d$  corresponds to the deformation potential and  $\gamma$  is the gruneisin constant. The value of the dielectric constant  $\epsilon$  is very close to literature values determined from far infrared spectroscopy experiments (see reference [2]). The electron effective mass of 2  $m_0$  is only an approximate value as the model was quite insensitive to the variations of  $m_n^*$ . It only confirms the experimental findings [1] that the electrons have much lower mobilities than holes in IrSb<sub>3</sub>.

Using this set of parameters, all thermoelectric properties of p-type IrSb<sub>3</sub> were recalculated as a function of carrier concentration (by varying the chemical potential) and temperature. The extrapolated values for the Hall mobility, the power factor, the thermal conductivity and the dimensionless figure of merit are plotted in figures 1 to 4 respectively.

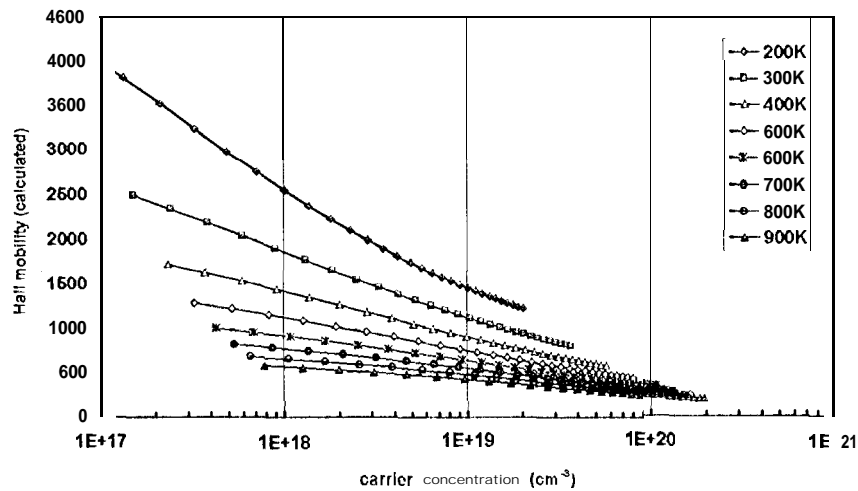


Figure 1: Calculated Hall mobility values as a function of carrier concentration at different temperatures for p-type IrSb<sub>3</sub>.

The temperature dependence of the Hall mobility is close to  $T^{-1.1}$  which indicates that the scattering of carriers by acoustic phonons is predominant. It is interesting to note that in the model calculations there is little or no minority carrier effects even at the lowest carrier concentration levels, due to the heavy electron effective mass. Experimental data has consistently shown an important decrease in mobility for carrier concentrations lower than  $6$  to  $7 \times 10^{18} \text{ cm}^{-3}$  [1]. Attempts to understand and reconcile these differences have not been successful and more experimental analysis is required.

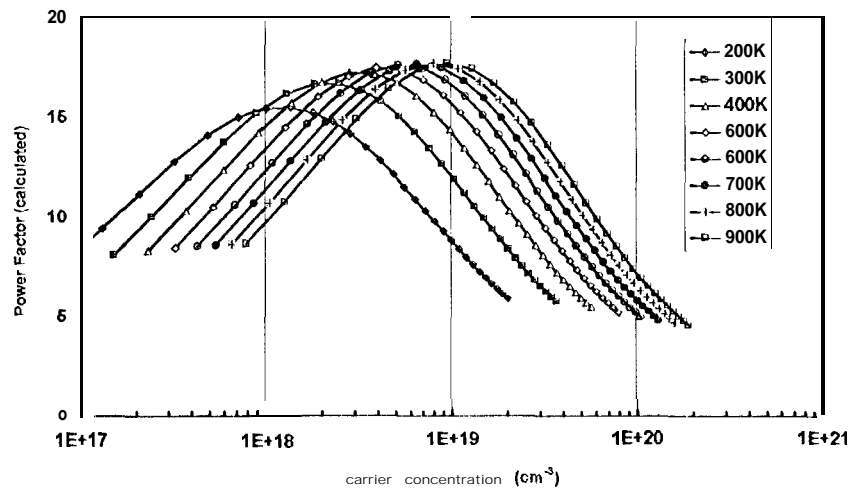


Figure 2: Calculated power factor values as a function of carrier concentration at different temperatures for p-type IrSb<sub>3</sub>.

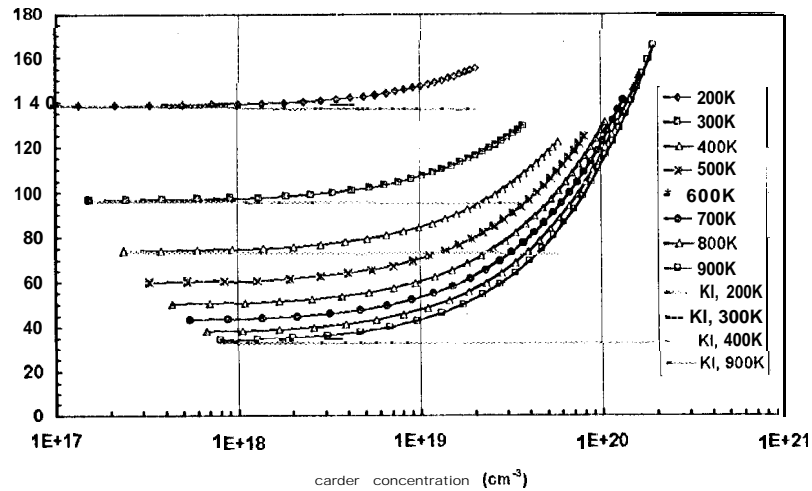


Figure 3: Calculated total thermal conductivity values as a function of carrier concentration at different temperatures for p-type IrSb<sub>3</sub>. The calculated lattice contribution is also displayed for a few temperatures.

A slow increase in both maximum power factor and optimum doping level can be observed in Figure 2. The lattice contribution to the thermal conductivity has been plotted in Figure 3 for a few temperatures. It is clear that it is the dominant term in p-type IrSb<sub>3</sub>, contributing about 90% for a carrier concentration of 10<sup>19</sup> cm<sup>-3</sup>. Also, the very small decrease of the lattice thermal conductivity with increasing carrier concentration indicates that the hole-phonon scattering mechanism is very weak and phonon-phonon processes dominate.

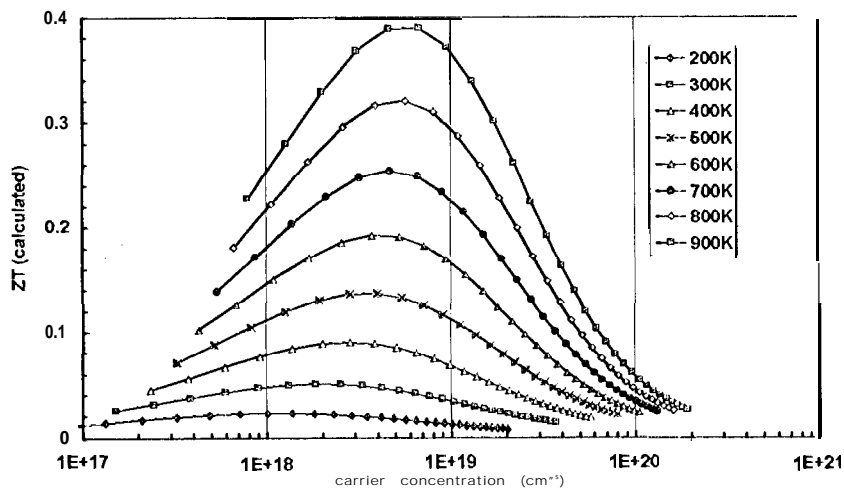


Figure 4: Calculated ZT values as a function of carrier concentration at different temperatures for p-type IrSb<sub>3</sub>.

Finally, the variations of  $ZT$  with carrier concentration and temperature reproduced in Figure 4 show that the best values are obtained at high temperatures, with a maximum value of 0.4 at 900K. These findings are very close to the experimental results [1] obtained on p-type  $\text{IrSb}_3$  samples which were not heat-treated. This increase in  $ZT$  is consistent with the large band gap value of 1.18 eV and high peritectic decomposition temperature of 1141°C. However, experimentally, higher temperatures (above 1050 K) have resulted in partial decomposition of  $\text{IrSb}_3$  samples and use of this material above 1000K would be difficult.

## ADDITION OF PHONON SCATTERING CENTERS

Additions of randomly distributed ultrafine particulates into an otherwise undisturbed single crystalline thermoelectric material have been suggested as a possible mechanism to scatter intermediate wavelength phonons and decrease the lattice thermal conductivity. Calculations performed for Si-Ge alloys [3-5] determined that 10 to 40% improvement in the figure of merit  $Z$  might be obtained. Experimental work conducted on hot-pressed p-type Si-Ge alloys with additions of BN particulates 50Å in diameter successfully demonstrated the enhanced phonon scattering rate [9]. A similar approach was applied to the calculation of the changes in lattice thermal conductivity of  $\text{Bi}_2\text{Tc}_3$ -based alloys by introducing inert scattering centers and determined that a maximum improvement of 20% could be obtained at low temperatures [7]. This theoretical framework is now applied to p-type  $\text{IrSb}_3$  to assess the impact of adding inert scattering centers such as voids on the thermal and electrical transport properties in a 200-900 K temperature range.

### Lattice Thermal Conductivity

Calculation of the lattice thermal conductivity was carried out by adding scattering by ultrafine electrically and thermally insulating inclusions to the three other scattering mechanisms already considered by the model. The new total phonon scattering rate is determined from (3):

$$\frac{1}{\tau_c} = \frac{1+\beta}{\tau_u} + \frac{1}{\tau_{pd}} + \frac{1}{\tau_e} + \frac{1}{\tau_{sc}} \quad (3)$$

where  $\tau_{sc}$  is the relaxation time due to ultrafine scattering centers. Assuming a spherical inclusion, the expression for the phonon relaxation time is [8]:

$$\frac{1}{\tau_{sc}} = NA v \quad (4)$$

where  $N$  corresponds to number of inclusions per unit volume and  $A$  is the cross-sectional area of the inclusions. Rewriting (4) in terms of  $c$ , the volume fraction of inclusions, and  $d$ , their diameter:

$$\tau_{sc} = \frac{3cv}{2d} \quad (5)$$

This expression indicates that the smaller the diameter and the larger the volume fraction of inclusions, the higher the scattering rate and thus the lower the lattice thermal conductivity.

### Electrical transport properties

Corrections to the bulk transport properties can be estimated, by considering theoretical work done on the transport properties of heterogeneous materials. Expressing the effective electrical conductivity  $\sigma$  as a Fourier series about the volume-averaged value and considering an isotropic medium in which the variations in electrical conductivity have no preferred direction [10, 11], one obtains the following expression

$$\sigma = \sigma_0 \left[ 1 - \frac{1}{3} \frac{\langle \Delta\sigma^2 \rangle}{\sigma_0} \right] \quad (6)$$

where  $\sigma_0$  is the volume-averaged value and  $\langle \Delta\sigma^2 \rangle$  corresponds to an integrated average of the variations in conductivity. Considering a composite material consisting of a continuous matrix of IrSb<sub>3</sub> of electrical conductivity  $\sigma_{IrSb}$  and of ultrafine scattering inclusions of electrical conductivity  $\sigma_{sc}$ , (6) can be rewritten as:

$$\sigma = \sigma_{BiTe} \left( 1 - \frac{4c}{3} \right) \quad (7)$$

From (7), it is clear that the larger the volume fraction of the inclusions, the larger the decrease in electrical conductivity. Using a similar approach considering perfect thermal insulators, an analogous relationship is obtained for the thermal conductivity:

$$\lambda = \lambda_{BiTe} \left( 1 - \frac{4c}{3} \right) \quad (8)$$

To estimate the correction to the Seebeck coefficient, exact calculations [12] relating to the thermoelectric transport properties of composite materials were used. Assuming once again perfect electrically and thermally insulating inclusions, it can be shown that:

$$S \approx S_{BiTe} \quad (9)$$

So, in the case of perfect electrical and thermal insulators such as voids, corrections to the electrical and thermal conductivity cancel each other in the expression of ZT. An identical end result is obtained in the case of perfectly electrically and thermally conducting inclusions, by calculating the perturbations on the electrical and thermal resistivity this time [11].



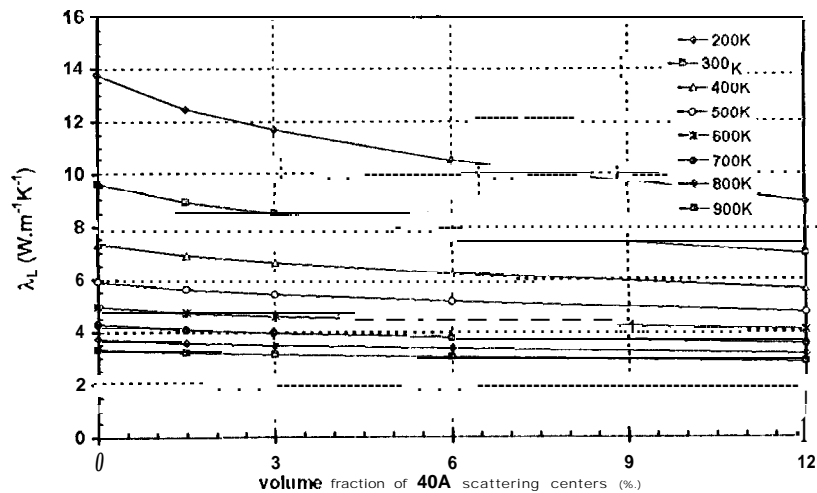


Figure 5: Calculated lattice thermal conductivity values as a function of the volume fraction of inert scattering inclusions for p-type  $\text{IrSb}_3$ . The inclusions are  $40\text{\AA}$  in diameter and the carrier concentration was selected at the optimum doping level.

To illustrate the model results, the lattice thermal conductivity and dimensionless figure of merit values calculated as a function of the volume fraction of inert scattering inclusions for p-type  $\text{IrSb}_3$  have been plotted in Figure 5 and 6 respectively. In both cases, the inclusions are  $40\text{\AA}$  in diameter and the carrier concentration was selected at the optimum doping level (giving maximum  $ZT$ ). Figure 5 shows that the lattice thermal conductivity could be substantially reduced at low temperatures, by up to 50%. However, this decrease becomes much less significant at high temperatures where the lattice thermal conductivity is already reasonably low. This behavior results in improvement in maximum  $ZT$  (Figure 6 shows relative increases). For the highest volume fractions of inclusions,  $ZT_{\text{max}}$  actually decreases at high temperatures as the degradation in electrical properties overwhelms the reduction in thermal conductivity.

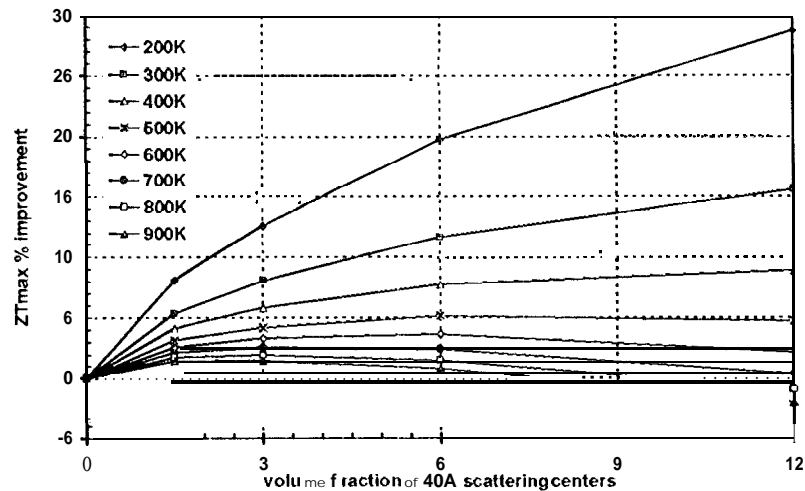


Figure 6: Calculated relative improvement in maximum  $ZT$  (optimum doping level) with increasing volume fraction of inert scattering inclusions for p-type  $\text{IrSb}_3$ . The inclusions are  $40\text{\AA}$  in diameter and the degradation in electrical properties was taken into account.

## RESONANT SCATTERING OF CARRIERS

Resonant scattering of the charge carriers has been considered extensively for IV-VI semiconductors such as  $\text{PbTe}$  and  $\text{PbSe}$  [13]. Theoretical analysis of the variations of the carrier mobility and Seebeck coefficient of these materials when doped with impurities such as  $\text{In}$  and  $\text{Tl}$  have shown that the anomalous increase in power factor at high doping levels could be interpreted by introducing an additional scattering mechanism for the charge carriers called resonant scattering [13, 14]. This overall improvement in electrical properties is due to the reduction in the contribution of “cold” charge carriers to the Seebeck coefficient. For a heavily degenerated semiconductor ( $\zeta > 0$ ), these “cold” carriers of lower energy than the chemical potential ( $x < \zeta$ ) have a negative contribution to the Seebeck coefficient while “hot” carriers of higher energy than the chemical potential ( $x > \zeta$ ) have a positive contribution to the Seebeck coefficient. By selectively scattering the cold charge carriers the substantial enhancement in the Seebeck coefficient will more than offset the corresponding decrease in electrical conductivity and result in an improved  $ZT$  (the total thermal conductivity will also decrease due to the reduction in electronic thermal conductivity). The development of this type of scattering mechanism for achieving high  $ZT$  values has been advocated for  $\text{Bi}_2\text{Te}_3$ -based alloys and for  $\text{Bi-Sb}$  alloys [15]. Because  $\text{IrSb}_3$  samples were found to be also heavily degenerated, it was found of interest to analytically explore such possibilities using published expressions for the resonant scattering rate. If we consider the existence of a band of resonant impurities centered in energy at  $\xi_{\text{res}}$

and of width  $\Gamma$  (expressed in  $kT$  units) then the resonant scattering relaxation time can be written as [15]:

$$\frac{1}{\tau_{\text{res}}} = \frac{1}{\tau_{\text{res}}^0} \left[ 1 + \left( \frac{\xi - \xi_{\text{res}}}{\Gamma/2} \right)^2 \right] \quad (10)$$

where  $\frac{1}{\tau_{\text{res}}^0}$  represents the maximum strength of the resonant scattering rate relative to the rate obtained for acoustic phonon scattering of the charge carriers.

Using the set of transport parameters obtained after successful y fitting the experimental data, the electrical properties (Hall mobility, electrical conductivity and Seebeck coefficient) were recalculated as a function of carrier concentration and temperature using various sets of values for  $\xi_{\text{res}}$ ,  $\Gamma$  and  $\frac{1}{\tau_{\text{res}}^0}$ . The large number of variables (a total of five) made difficult the determination of the optimum values for the three resonant scattering parameters, g'bus, it was decided to fix the temperature and two of the parameters and vary carrier concentration and the last parameter. A number of 3 dimensional plots showing the changes of the electrical properties with these two variables were constructed. Figures 7 to 9 illustrate this process and help understand the trends in the variations of the Hall mobility, the Seebeck coefficient and the power factor.

On Figure 7, the line labeled "N" shows the decrease of the Hall mobility with increasing carrier concentration at  $500^\circ\text{C}$  in the absence of any resonant impurity band. The other lines of the 3 dimensional surface plot the variations of the mobility with carrier concentration when a resonant impurity band of  $0.5kT$  in width and with a maximum scattering rate 5 times stronger than the acoustic phonon scattering rate moves from  $0kT$  (top of the valence band in p-type  $\text{IrSb}_3$ ) to  $10kT$  (inside the valence band). It can be seen that there is a substantial drop in mobility associated with the chemical potential (and thus the carrier concentration) being near or at the center of the resonant band. As the resonant band moves deeper into the valence band, the perturbation is displaced to higher carrier concentrations. It is interesting to note that the relative decrease in mobility is smallest at high carrier concentrations and deep resonant bands.

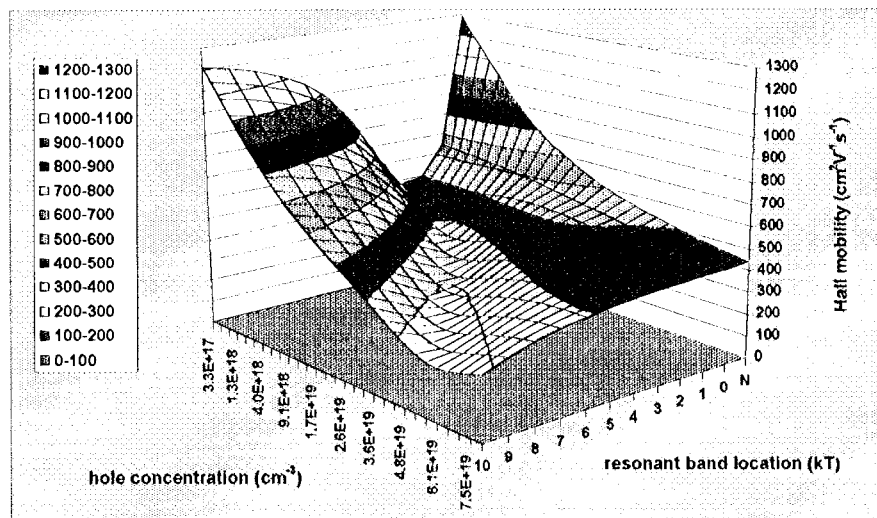


Figure 7: Calculated Hall mobility values at 500°C as a function of carrier concentration and for different energy locations of the center of the resonant impurity band.

On Figure 8, the line labeled “O” shows the decrease of the Seebeck coefficient with increasing carrier concentration at 500°C in the absence of any resonant impurity band (zero strength). The other lines of the 3 dimensional surface plot the variations of the Seebeck coefficient with carrier concentration when a resonant impurity band of 0.5kT in width and located at 10 kT inside the valence band of p-type IrSb<sub>3</sub> has a maximum scattering rate 1 time to so times stronger than the acoustic phonon scattering rate. It can be seen that there is an abrupt variation in Seebeck coefficient associated with the chemical potential being near or at ‘the center of the resonant band. For values of the chemical potential lower than  $\xi_{res}$  the positive hot carrier contribution is quenched and the Seebeck values become very small or even negative. Use of this effect was suggested to obtain p-type Bi-Sb thermoelectric alloys [15]. On the other hand, for values of the chemical potential higher than  $\xi_{res}$  the negative cold carrier contribution is quenched and the Seebeck values become up to 5 times larger than in the absence of resonant impurities.

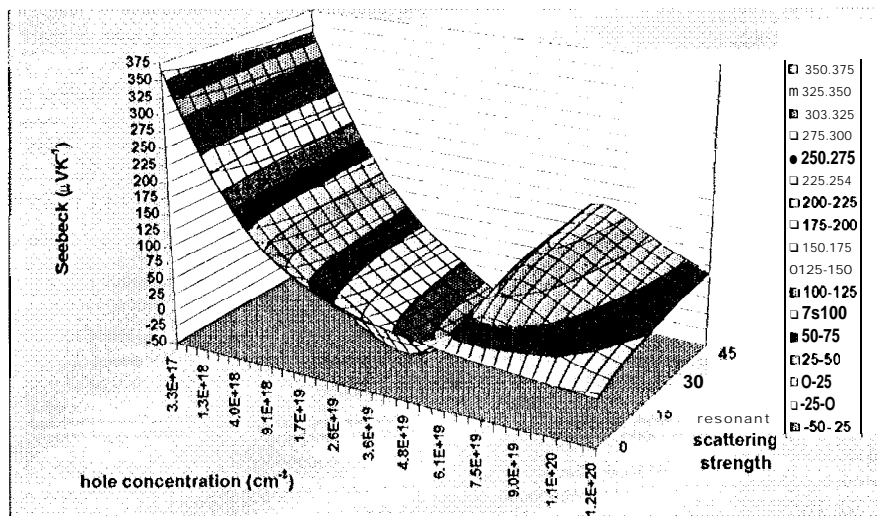


Figure 8: Calculated Seebeck coefficient values at  $500^\circ\text{C}$  as a function of carrier concentration and for different strengths of the resonant scattering (relative to the acoustic phonon scattering rate)

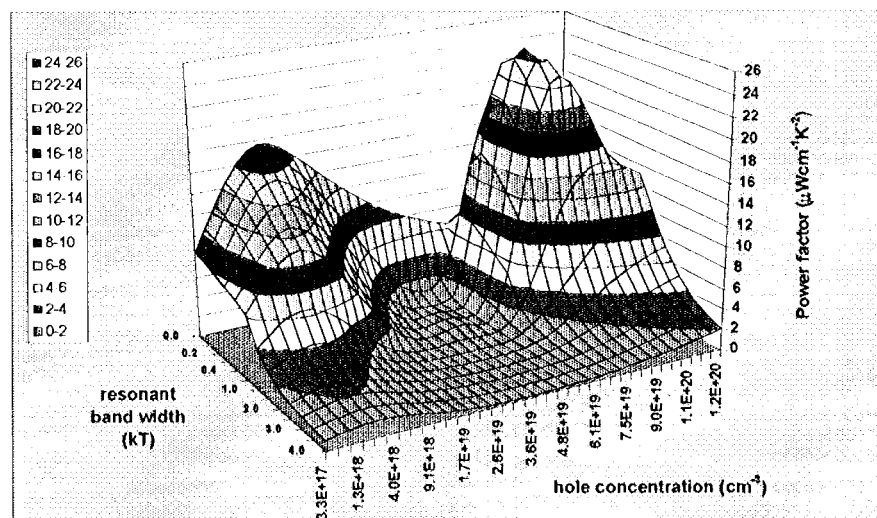


Figure 9: Calculated power factor values at  $500^\circ\text{C}$  as a function of carrier concentration and for different bandwidths of the resonant impurity band.

On Figure 9, the line labeled “O” shows the decrease of the power factor with increasing carrier concentration at  $500^\circ\text{C}$  in the absence of any resonant impurity band (zero width). The other lines of the 3 dimensional surface plot the variations of the power factor with carrier concentration when a resonant impurity band located at  $10\text{ kT}$  inside the valence band of p-type  $\text{IrSb}_3$  and with a maximum scattering rate 15 times stronger than the acoustic phonon scattering rate has a bandwidth which varies from  $0.1$  up to  $4\text{ kT}$ . An optimal combination of the three parameters of the resonant impurity band in p-type  $\text{IrSb}_3$  is obtained for a bandwidth of  $0.3\text{ kT}$  and a carrier concentration of about  $1020\text{ cm}^{-3}$ . This corresponds to a maximum fivefold increase in power factor over p-type  $\text{IrSb}_3$  without resonant impurities and at the same doping level. However, this is only  $50\%$

higher than the value obtained at the optimum doping level. Furthermore, in the case of p-type IrSb<sub>3</sub>, the very high carrier concentrations required for an efficient resonant scattering bring a high thermal conductivity value, about 9.2 W.m<sup>-1</sup>K<sup>-1</sup> at 300K. This value is substantially higher than the 6.4 W.m<sup>-1</sup>K<sup>-1</sup> obtained at the optimum doping level in the absence of resonant impurities. This means that the gain in power factor is offset by the corresponding increase in thermal conductivity, resulting in little or no improvement in ZT. Calculations performed at various temperatures qualitatively showed no difference with these findings.

## CONCLUSION

A good agreement between experimental and calculated data ( $\pm 20\%$ ) was achieved by considering a one valence band, one conduction band model for p-type IrSb<sub>3</sub>. Results show that a maximum ZT value of 0.4 can be obtained at 900K. Additional calculations were performed to investigate the possibility of improving ZT by adding inert scattering centers and reduce the lattice thermal conductivity or by adding resonant scattering centers and enhance the Seebeck coefficient. Both approaches show that at best marginal improvements will be achieved. Other mechanisms need to be considered in order to obtain high ZT values. Several skutterudite compounds such as IrSb<sub>3</sub> have exceptionally high p-type mobilities but rather high thermal conductivity and moderate Seebeck coefficient. The study of more complex compositions with the skutterudite structure and based on IrSb<sub>3</sub> offer interesting possibilities and are currently being studied at JPL.

## ACKNOWLEDGMENTS

The work described in this paper was carried out by the Jet Propulsion Laboratory/ California Institute of Technology, under a contract with the National Aeronautics and Space Administration.

## REFERENCES

1. Caillat, T., Borshchevsky, A., and Fleurial, J.-P., "Preparation and Thermoelectric Properties of p and n-Type IrSb<sub>3</sub>", this conference.
2. Slack, G. A., and Tsoukala, V. G., J. Appl. Phys. (to be published).
3. Vining, C. B., "A Model for the High Temperature Transport Properties of Heavily Doped n-type Silicon-Germanium Alloys", J. Appl. Phys., 69 (1), 331-341 (1991).
4. Vining, C.B., "A Model for the High Temperature Transport Properties of Heavily Doped p-type Silicon-Germanium Alloys", in *Modern Perspectives on Thermoelectrics and Related Materials*, MRS Symp. Proc. Vol. 234, 95-104, (Materials Research Society, Pittsburgh, Pennsylvania 1991).
5. Fleurial, J.-P., "Thermal and Electrical Transport Properties Modeling of Bi<sub>2</sub>Tc<sub>3</sub>-Based Alloys with Addition of Ultrafine Scattering Centers", in

*Proceedings of the XI<sup>th</sup> International Conference on Thermoelectrics*, 1992, Arlington, Texas, USA, October 7-9, pp. 276-281.

6. Fleurial, J.-P., and Borshcheysky, A., "Properties of Semiconducting  $Ru_2Ge_3$ ", *Proceedings of the XII<sup>th</sup> International Conference on Thermoelectrics*, 1993, Yokohama, Japan, November 9-11, pp. 236-241.
7. Fleurial, J.-P., "Evaluation of the Improvement in the Figure of Merit of  $13i_2Tc_3$ -based alloys", *Proceedings of the XII<sup>th</sup> International Conference on Thermoelectrics*, 1993, Yokohama, Japan, November 9-11, pp. 1-6.
8. White, D. P., and Klemens, P. G., "Thermal conductivity of thermoelectric  $Si_{0.8}Ge_{0.2}$  alloys", *J. Appl. Phys.*, 71 (9), 4258 (1992).
9. Beaty, J. S., Rolfe J.L., and Vandersande, J. W., "Thermoelectric Properties of Hot-Pressed Ultrafine Particulate Si-Ge Powder Alloys with Inert Additions", in *Modern Perspectives on Thermoelectrics and Related Materials*, MRS Symp. Proc. Vol. 234, 105-109, (Materials Research Society, Pittsburg, Pennsylvania 1991).
10. Klemens, P. G., *Thermal Conductivity 21*, Edited by C.J. Cremers and H.A. Fine, Plenum Press, New York, 1991, "Thermal Conductivity of Inhomogeneous Materials", pp. 383-390.
11. Klemens, P. G., "Electrical resistivity of inhomogeneous alloys", *J. Appl. Phys.*, 70 (8), 4322 (1991).
12. Bergman, D. J., and Levy, O., "Composite Thermoelectrics-Exact Results and Computational Methods", in *Modern Perspectives on Thermoelectrics and Related Materials*, MRS Symp. Proc. Vol. 234, 39-45, (Materials Research Society, Pittsburg, Pennsylvania 1991).
13. Kaidanov, V. I., Nemov, S. A., and Ravich, Yu.I., "Resonant Scattering of Carriers in IV-VI Semiconductors", *Sov. Phys. Semicond.*, 26 (2), 113-123 (1992)
14. Ravich, Yu. I., "Selective Scattering in Thermoelectric Materials", to be published in CRC Handbook on Thermoelectrics.
15. Ravich, Yu. I., and Vedernikov, M. V., "On a Possibility of increasing the Thermoelectric Figure of Merit Through Resonance Charge Carrier Scattering", *Proceedings of the IX<sup>th</sup> International Conference on Thermoelectrics*, 1990, Pasadena, CA, USA, March 19-21, pp. 278-295.